Received: 30 December 2023 | Revised: 16 February 2024 | Accepted: 8 March 2024

DOI: 10.1111/php.13940

RESEARCH ARTICLE

Compound collagen peptide powder improves skin photoaging by reducing oxidative stress and activating TGF-β1/Smad pathway

Kaien Guo[1] | Linxin Zheng[1,2] | Xin Zeng[1] | Guangchun Huang[3] | Lingling Meng[1] | Yuting Yin[4]

[1]Department of Postgraduate, Jiangxi University of Chinese Medicine, Nanchang, China

[2]Formula pattern Research Center, Jiangxi University of Chinese Medicine, Nanchang, China

[3]Jiangxi Wufang Biotechnology Co., Ltd, Nanchang, China

[4]College of Pharmacy, Jiangxi University of Chinese Medicine, Nanchang, China

Correspondence
Yuting Yin, College of Pharmacy, Jiangxi University of Chinese Medicine, 1688 Meiling Road, Nanchang 330004, Jiangxi Province, China.
Email: sandel@163.com

Funding information
1 Jiangxi College Students' Innovation and Entrepreneurship Training Program Project, Grant/Award Number: S202310412063;
2 Jiangxi Provincial Chinese Medicine Young and Middle-aged Backbone Talents (Fourth Batch) Training Program Project;
3 Jiangxi University of Chinese Medicine Science and Technology Innovation Team Development, Grant/Award Number: CXTD22007

Abstract

Fish collagen peptide (FCP) has been extensively investigated as a natural product that can combat photoaging; however, its efficacy is limited by its singular composition. Compound collagen peptide powder (CCPP) is a novel functional food formulation that exhibits photoprotective properties and comprises FCP and a blend of natural botanical ingredients. The objective of this study was to investigate the efficacy of CCPP and its molecular mechanism. CCPP had a low molecular weight, facilitating its efficient absorption, and was abundant in amino acids, total polyphenols, and total flavonoids. The results of in vivo studies demonstrated that CCPP exhibited significant efficacy in reducing skin wrinkles, enhancing the contents of water and oil in the skin, and ameliorating histopathological alterations in mice. The results of in vitro studies demonstrated that CCPP effectively mitigated photoaging in human skin fibroblasts by attenuating oxidative stress and promoting extracellular matrix (ECM) synthesis. Moreover, we clearly demonstrated that the TGF β1/Smad pathway was involved in the promotion of ECM synthesis and cell proliferation by CCPP in human skin fibroblasts. These findings suggest that, compared with single collagen, CCPP has a more comprehensive range of antiphotoaging properties.

KEYWORDS

compound collagen peptide powder, fish collagen peptide, oxidative stress, photoaging, TGF-β1/Smad pathway

INTRODUCTION

Sunlight ultraviolet (UV) irradiation is one of the main external factors causing skin damage, and long-term UV exposure is likely to cause dry and rough skin, sagging, inelasticity, wrinkles, and accelerated skin aging.[1] Collagen type 1 (COL1), elastin (ELN), and hyaluronic acid (HA) are important extracellular matrix (ECM) components in the dermis that are closely related to skin elasticity, luster, moisturizing properties, and tension. Skin exposure to UV irradiation results in a significant decrease in ECM content,[2] which is a direct contributor to skin photoaging. Fibroblasts are the most abundant cells in the dermis and

Straive | Journal Name PHP | Manuscript No. 13940 | WILEY | No. of pages: 19 | Dispatch: 15-3-2024 | PE: | CE:

are responsible for the production and secretion of ECM to maintain the normal structure and function of the dermis.[3] However, under UV irradiation, fibroblasts aging and apoptosis can be accelerated, and their cellular activity is reduced, leading to a decreased synthesis of ECM.[4] Furthermore, Reactive oxygen species (ROS) have long been shown to be closely related to the aging process of cells,[5] and photoaging is no exception. When the skin is exposed to UV radiation, excess ROS are produced.[6] ROS impairs antioxidant enzymes, leading to oxidative stress in tissues and cells, which damages collagen and elastic fibers in the skin.[7,8]

Therefore, scavenging ROS and replenishing the dermis play key roles in delaying skin photoaging. Collagen peptide is an extensively studied and widely employed bioactive substance in the domain of skin anti-photoaging. It has been noted that collagen peptides from fish can reduce skin photoaging by improving skin hydration, increasing the levels of ECM components, reducing hyperpigmentation, and scavenging ROS.[9,10] Moreover, diverse botanical sources offer a plethora of natural bioactive compounds, including vitamins,[11,12] polyphenols,[13] polysaccharides,[14] and flavonoids,[15] which exhibit potent antioxidant properties and contribute to anti-aging effects by effectively scavenging free radicals. In current research, single collagen peptides are widely used and researched, but these studies have the disadvantage of using only a single raw material, which has an individual effect and a relatively limited improvement on skin photoaging. As a result, we have explored the incorporation of natural plant ingredients into collagen peptides, improving the single chemical property of collagen peptides and enhancing their resistance to anti-photoaging function.

Acerola is rich in vitamin C, fructose, and a variety of phenolic compounds with high antioxidant capacity, and their extracts and derivatives can reduce skin photoaging symptoms by reducing pigmentation, enhancing hydration, and increasing ECM content.[16–18] Broccoli is rich in vitamins, minerals, fiber, and a variety of phenolic compounds,[19] and the active ingredient sulforaphane can effectively reduce photoaging of human skin by improving pigmentation and reducing matrix metalloproteinase 1 (MMP 1) expression levels.[20] Cherry blossoms mainly contain active ingredients such as anthocyanins, flavonoids, and multiple vitamins and minerals,[21] and their extract was able to exert antiphotoaging effects by attenuating oxidative damage in HaCaT cells and inhibiting apoptosis.[22] Acerola extract, broccoli extract, and cherry blossom extract contain diverse natural antioxidant ingredients and have a rich material basis to fight against skin photoaging, and some research has achieved good results. For this reason, we have incorporated acerola powder, broccoli powder, and cherry blossom powder into fish collagen peptide (FCP) to produce a compound collagen peptide powder (CCPP). Based on the above findings, CCPP has the theoretical basis of being able to improve skin photoaging, but there is a lack of experimental results to systematically elucidate its efficacy level and molecular mechanism.

In this study, we employed animal and cellular models of photoaging to assess the ameliorative effects and potential mechanisms of action of CCPP on skin photoaging, aiming to offer novel strategies for daily protection against skin photoaging.

MATERIALS AND METHODS

Chemicals and reagents

All chemicals and standards were analytical grade. The gallic acid standard was obtained from Solarbio (Beijing, China). Rutin standard was obtained from MANST Biotechnology Co. (Sichuan, China). Hematoxylin–Eosin (HE) tissue staining solution was purchased from Leagene Inc. (Beijing, China). High glucose Dulbecco's modified Eagle medium (DMEM H) was purchased from Procell Life (Wuhan, China). Fetal bovine serum (FBS) was purchased from Sigma Aldrich (St. Louis, Missouri, USA). A cell proliferation assay kit was purchased from Keygen (Nanjing, China). Total RNA Extraction Kit, Sprint reverse transcription kit, and realtime PCR with SYBRgreen kit were purchased from Mei5 Biotechnology Co., Ltd (Beijing, China). Senescence-associated β galactosidase (SA β gal) staining kit was purchased from Solarbio (Beijing, China). The ROS assay kit was purchased from Beyotime (Shanghai, China). ELISA kits for COL1 (No. MM 0174H1), ELN (No. MM 4054H1), HA (No. MM 0438H1), SOD (No. MM 0390H1), GSH Px (No. MM 0457H1), MDA (No. MM 2037H1) were purchased from Jiangsu Meimian Industrial Co., Ltd (Jiangsu, Yancheng, China). Anti-TGF β1 (No. ab179695), anti-TGF βR2 (No. ab259360), anti-Smad2 (No. ab280888), anti-Smad3 (No. ab208182), anti-Smad2/3 (No. ab272332), anti-GAPDH (No. ab199553), and Goat anti-Mouse IgG (HRP) (No. ab205719) were purchased from Abcam (Waltham, MA, USA). Goat anti-Rabbit IgG (HRP) (No. AS014) was purchased from ABclonal (Wuhan, China). LY2109761 was purchased from MCE (New Jersey, USA).

Materials

Fish collagen peptide (FCP) (extracted from the skin of a deep sea cod) was obtained from Rousselot Inc. (Paris, France). Acerola powder was purchased from Nexira

Inc. (Fleurbaix, France). Broccoli powder and Kwanzan cherry blossom powder were purchased from Oryza Inc. (Tokyo, Japan).

Preparation of CCPP

Compound collagen peptide powder (CCPP) was produced by Jiangxi Wufang Biotechnology Co., Ltd. to good manufacturing practice requirements. CCPP is an oral functional food prepared by mixing fish collagen peptide (FCP) (Rousselot, Paris, France) as the main raw material and acerola powder (Nexira, Fleurbaix, France), broccoli powder (Oryza, Tokyo, Japan) and Kwanzan cherry blossom powder (Oryza, Tokyo, Japan) as auxiliary ingredients. Each 10 g of finished CCPP contained 5 g of FCP, 2 g of acerola powder, 2 g of broccoli powder, and 1 g of Kwanzan cherry blossom powder. The dry ingredients were precisely weighed and added to a food blender (Supor, Hangzhou, China) for thorough mixing. Preparation and storage were carried out within the temperature range of 20 ± 5°C and a relative humidity between 45% and 60%.

Molecular weight distribution analysis

The molecular weight distribution of CCPP was analyzed using gel permeation chromatography (GPC) with an Agilent 1260 Infinity System (Agilent Technologies, Pittsburgh, PA, USA). One gram of CCPP was dissolved in 10 mL of ultrapure water and subsequently passed through a 0.22 μm aqueous microporous filter membrane before injection for retention time analysis. A TSK GEL G2000SWXL chromatographic column (7.8 mm × 30.0 cm) (Tosoh Bioscience, Tokyo, Japan) was utilized for the experiment. The mobile phase, 30% acetonitrile with 0.1% trifluoroacetic acid (TFA), was utilized at a flow rate of 0.5 mL/min, and an injection volume of 20 μL was used. The UV detection wavelength was set at 220 nm, and the column temperature was maintained at 40°C.[23]

Amino acid content analysis

First, 150 mg of CCPP was accurately weighed to which 15 mL of 6 M hydrochloric acid and 0.2 g of phenol were added, and the mixture was sealed immediately after vacuum extraction and hydrolyzed at 110°C for 22 h. After hydrolysis, the mixture was removed, cooled to room temperature, redissolved in 10 mL of 0.1% formic acid, filtered through a 0.22 μm membrane, and analyzed using a fully automated amino acid analyzer (L8900 series, Hitachi, Tokyo, Japan) with detection wavelengths of 440 and 570 nm.[24]

Quantification of the total polyphenol content (TPC) and total flavonoid content (TFC)

Quantification of the TPC in CCPP and FCP was performed using the Folin method.[25] A gallic acid extract was prepared as a standardized solution at a range of concentrations, and the corresponding absorbance values were determined and utilized for constructing a standard curve. Then, precisely 3 g of CCPP or FCP were added to 30 mL of 60% ethanol, and the solution was subsequently subjected to sonication for 10 min. The mixture obtained was subsequently subjected to filtration and then mixed with a reagent consisting of 10% Folin phenol, and a solution containing 10% sodium carbonate, followed by incubation in a water bath at 37°C for 50 min. The absorbance was measured at 750 nm using a UV–visible spectrophotometer (Thermo Fisher, Wilmington, Massachusetts, USA). Finally, the TPC was determined by employing the calibration curve. Quantification of the TFC in CCPP and FCP was performed using a modified UV spectrophotometry method.[26] First, 10 mg of rutin was added to methanol in a 50 mL volumetric flask, ensuring that the volume was adjusted accordingly. Various quantities of the reference solution were precisely measured and transferred to individual 25 mL volumetric flasks. Next, 1 mL of a 5% sodium nitrite solution was added to each of these flasks, and the mixture was allowed to rest for 6 min. Afterward, 1 mL of a 10% aluminum nitrate solution was added, and the reaction was allowed to proceed for an additional 6 min. Subsequently, 10 mL of a 1% sodium hydroxide solution was added, and the mixture was vigorously mixed and left undisturbed for 15 min. CCPP and FCP were treated in a similar fashion. The absorbance of each sample was then measured at 510 nm. The above analysis was repeated three times.

Animal experiment

A total of 40 female-specific pathogen-free (SPF) ICR mice (6–8 weeks old, weighing 20 ± 2 g) were purchased from Slaughter Jingda Laboratory Animal Co., Ltd. (Changsha, Hunan, China) [Animal Certificate License SCXK (Xiang) 2019–0004]. The experiments were started after 5 days of acclimatization feeding in the SPF class animal room at the Experimental Animal Science and Technology Center of the Jiangxi University of Chinese Medicine. During the experiment, mice were given free access to food and

water, and the feeding room was illuminated for 12 h and darkened for 12 h. The room temperature was 22–24°C with constant humidity. This experiment was approved by the Experimental Animal Ethics Committee of the Jiangxi University of Chinese Medicine, with approval number JZLLSC20220757.

The mice were randomly divided into the following 4 groups ($n = 10$/group): (i) the Control group, not irradiated with UV light; (ii) the UV group, irradiated with UV light; (iii) the compound collagen peptide powder (CCPP) group, irradiated with UV light and treated with CCPP (200 mg kg^{-1} body weight); and (iv) the fish collagen peptide (FCP) group, irradiated with UV light and treated with FCP (200 mg kg^{-1} body weight). Before administration, CCPP and FCP were dissolved in saline. All the mice were treated for back skin removal 24 h before the first UV exposure. The hair on the backs of the mice was carefully removed using a depilatory cream to form a bare area (5 × 3 cm). Mice in the CCPP and FCP groups were administered CCPP and FCP within 1 h before UV exposure. The Control and UV groups were administered equal volumes of saline. The UV light source was a benchtop UV irradiator (SIGMA, Shanghai, China) with a UVA intensity of 6.7 mW cm^{-2} and UVB intensity of 0.45 mW cm^{-2}. The distance from the UV light source to the back of the mice was 25 cm, and the mice were irradiated once a day, 5 days a week, for a total of 9 weeks, except for the mice in the Control group. The total UVA and UVB irradiation doses were 94.5 and 9.45 J cm^{-2} for the whole experimental cycle, respectively.[27]

Overall efficacy in mice and histopathological analysis

Twenty four hours after the last UV irradiation treatment, the water content and oil content of the dorsal skins of the mice were measured using a smart skin detector (Belulu, Yokohama, Japan). The measurement was repeated 3 times, and the average value was taken. Moreover, images of the backs of the mice were acquired. Mice were anesthetized by intraperitoneal injection of 1% pentobarbital sodium at a dose of 80 mg kg^{-1} and then sacrificed. The central skin on the back was isolated for further analysis.

After 3 days of fixation using 4% paraformaldehyde, the skin tissue was cut longitudinally into 3–4 mm tissue blocks using a scalpel blade, dehydrated with a gradient of ethanol concentrations, made transparent with xylene, and then paraffin embedded. The samples were then cut into 5 μm thick sections for hematoxylin–eosin (HE) staining. Images were taken by light microscopy (Lecia, Wetzlar, Germany).

Cell culture

Human skin fibroblast BJ cells were obtained from American Type Culture Collection (Manassas, Virginia, USA), cultured in DMEM H containing 10% FBS and 1% penicillin–streptomycin in a 37°C, 5% CO_2 cell culture incubator. Cell morphology was observed daily, and the culture medium was changed once every 2 days. When cell confluence reached 80%–90%, the cells were digested with 0.25% trypsin and passaged 1:2. All experiments used active BJ cells from generations 3–5.

Cell photoaging model and treatment

When cell confluence reached 80%–90%, a single cell suspension was collected after 0.25% trypsin digestion, and the cell density was adjusted to 1×10^5 mL^{-1}. The cells were then added to well plates and cultured for 24 h. In this experiment, the cells were divided into the Control group, the UVA group (30 J cm^{-2} UVA irradiation), the CCPP H group (high concentration of CCPP, 12.50 mg mL^{-1}), the CCPP M group (medium concentration of CCPP, 6.25 mg mL^{-1}), the CCPP L group (low concentration of CCPP, 3.13 mg mL^{-1}), the FCP group (6.25 mg mL^{-1} FCP), the UVA + LY2109761 group (pretreatment with 5 μM LY2109761 followed by 30 J cm^{-2} UVA irradiation), and the CCPP H + LY2109761 group (pretreatment with 5 μM LY2109761 followed by 30 J cm^{-2} UVA irradiation and administration of 12.50 mg mL^{-1} CCPP). Before administration, CCPP and FCP were dissolved in DMEM H. Except for those in the control group, the cell media in all groups was first replaced with the same volume of phosphate-buffered saline (PBS), and then the cells were exposed to UVA irradiation. The UVA light source was a benchtop UVA irradiator (RCLH, Beijing, China) with a UVA intensity of 200 mW cm^{-2}. The distance between the UVA light source and the cells was 15 cm.[28] After irradiation, the cells in all groups were washed once with PBS. Immediately, the conventional medium was added to the Control group and UVA group, the CCPP H, CCPP M, and CCPP L groups were treated with 12.50, 6.25, and 3.13 mg mL^{-1} CCPP medium, respectively, and the FCP group was treated with 6.25 mg mL^{-1} FCP medium for 24 h.

Cell viability assay

Cell viability was assayed using a CCK 8 kit. BJ cells (1×10^4/well) were inoculated in 96 well plates. Cells without any treatment were first exposed to different doses of UVA [0 (unirradiated), 5, 10, 20, or 30 J cm^{-2}],

and cell viability was measured after 24 h of incubation according to the kit instructions to determine the appropriate UVA dose for modeling. Then, we performed toxicity tests with CCPP and FCP with BJ cells by culturing the cells without any UV treatment in different concentrations of CCPP and FCP for 24 h. Cell viability was measured in the same way, and the concentration of each peptide that had no toxic effect on the cells was selected for this experiment.

After the UVA irradiation dose and peptide administration concentration were determined, we performed treatment according to the aforementioned experimental groupings. Twenty four hours after the completion of UVA irradiation and the addition of CCPP and FCP medium, the cell viability in each group was measured according to the kit instructions. The above absorbance measurements were performed by a microplate reader (MD, San Jose, USA).

Cell proliferation assay

Cell proliferation was assayed using a cell proliferation assay kit. BJ cells (2×10^5/well) were inoculated in 6 well plates, incubated for 24 h, and then treated according to the experimental groupings described previously. The cells were collected by trypsin digestion in 1.5 mL tubes and centrifuged at 300×*g* for 5 min. Then, the cells were resuspended and gradually supplemented with pre-cooled anhydrous ethanol, followed by incubation at 4°C for 1 h. The cells were centrifuged again, and the supernatant was aspirated. Ki67 antibody was added for 1 h of incubation at room temperature. Subsequently, goat anti-rabbit IgG FITC was added for 30 min of incubation at room temperature. The completed incubated cells were transferred to flow tubes for detection using a flow cytometer (BD, Franklin Lakes, USA). The data analysis was conducted using FlowJo software V10 (TreeStar, Ashland, USA). Where needed, cells were pretreated with 5 μM TGF β receptor inhibitor LY2109761 for 2 h prior to UV irradiation treatment.

SA β gal staining

A senescence-associated β galactosidase (SA β gal) staining kit (Solarbio, Beijing, China) was used to assess cell aging. BJ cells (1×10^5/well) were inoculated in 24 well plates, and treatment was carried out as described above. The cell culture medium was aspirated, and the cells were washed once with PBS and then fixed and stained according to the kit instructions. The cells were then observed using an inverted microscope (Lecia, Wetzlar, Germany), and five fields of view were randomly selected to count the percentage of positive cells.[29]

Intracellular ROS level detection

A ROS assay kit was used to detect changes in ROS levels in the cells. BJ cells (1×10^5/well) were inoculated in 24 well plates, and treatment was carried out as described above. After aspiration of the medium, 500 μL of DCFH DA diluted in the medium at a ratio of 1:1000 (final concentration of 10 μM) was added to the wells in the plates according to the kit instructions and incubated for 30 min at 37°C in a cell incubator. Cell fluorescence was observed using an inverted fluorescence microscope (Lecia, Wetzlar, Germany). The average fluorescence intensity of DCF was quantified using ImagePro Plus 6.0 software (GraphPad Software, La Jolla, USA).

Enzyme-linked immunosorbent assay (ELISA)

The expression levels of SOD, GSH Px, MDA, COL1, ELN, and HA in BJ cells were measured using ELISA. BJ cells (2×10^5/well) were inoculated in 6 well plates, incubated for 24 h, and then treated according to the experimental groupings described previously. After washing the cells once with PBS, 100 μL of radioimmunoprecipitation assay (RIPA) buffer was added to each well for 30 min of incubation at 4°C. The cells were scraped with cell scrapers, and then the cell suspension was transferred to a 1.5 mL Eppendorf tube and repeatedly mixed with a pipette 30–60 times. After cell lysis, the cells were centrifuged at 4°C and 12,000 rpm for 5 min, and the total cell protein was collected by aspirating the supernatant. The expression levels of SOD, GSH Px, MDA, COL1, ELN, and HA in the cells were detected according to the ELISA kit instructions. Absorbance measurements were performed by a microplate reader (MD, San Jose, USA). Where needed, cells were pretreated with 5 μM TGF β receptor inhibitor LY2109761 for 2 h prior to UV irradiation treatment.

Western blot analysis

The protein expression levels of TGF β1, TGF βR2, Smad2, Smad3, and Smad2/3 in BJ cells were measured using Western blot. The total cellular protein was extracted according to the procedure for the ELISA method, and then the protein concentration was measured by the BCA (bicinchoninic acid) method. A 1/5 volume of 6× protein loading buffer was added to the total cell protein for incubation at 100°C for 15 min to denature the protein. Equal amounts of protein from each sample were electrically transferred to polyvinylidene difluoride (PVDF) membranes after the gels were separated by electrophoresis.

The PVDF membranes were blocked using a 5% bovine serum albumin (BSA) solution. PVDF membranes were incubated overnight at 4°C after adding primary antibodies diluted in the appropriate ratio, including TGF β1 (1:1000), TGF βR2 (1:500), Smad2 (1:1000), Smad3 (1:1000), Smad2/3 (1:500), and GAPDH (1:1000). The next day, the PVDF membranes were incubated in diluted goat anti-rabbit IgG (HRP) or goat anti-mouse IgG (HRP) at room temperature for 1 h. Subsequently, the membrane was transferred to a gel imager (Bio Rad, Hercules, USA) for exposure imaging. Grayscale values were analyzed using ImagePro Plus 6.0 software.

Quantitative real-time polymerase chain reaction (qPCR)

The mRNA expression levels of *COL1A1*, *COL1A2*, *ELN*, and *HAS2* in BJ cells were measured using qPCR. BJ cells (2×10^5/well) were inoculated in 6 well plates, incubated for 24 h, and then treated according to the experimental groupings described previously. Cells were washed once with PBS, and then total cellular RNA was extracted using the Total RNA Extraction Kit according to the manufacturer's instructions. The RNA concentration was measured by full wavelength zymography (MD, San Jose, USA). Total RNA was reverse transcribed to 500 ng of cDNA using the Sprint reverse transcription kit. Real-time PCR was performed on cDNA using the Real-time PCR with SYBRgreen kit according to the manufacturer's instructions. *GAPDH* was used as the housekeeping gene, and the relative expression level of each target gene was expressed using $2^{-\Delta\Delta Ct}$. The name and sequence of the primer are shown in Table 1.

Statistical analysis

SPSS 21.0 (IBM, Armonk, New York, USA) and GraphPad Prism 8.1 (GraphPad Software, La Jolla, California, USA) statistical analysis software were used to process the data. The measured data were expressed as the mean ± standard deviation (SD) and were analyzed by ANOVA combined with Dunnett's multiple comparison method; the count data were analyzed by the Kruskal–Wallis rank sum test. A value of $p < 0.05$ indicated that the difference was statistically significant.

RESULTS

Molecular weight distribution of CCPP

The GPC chromatogram in Figure 1 demonstrates that CCPP has two distinct molecular weight distributions. Table 2 lists the CCPP molecular weight assay results, which revealed number average molecular weights (Mn) of 2133 and 314 Da, weight average molecular weights (Mw) of 4696 and 330 Da, z mean molecular weights (Mz) of 11,289 and 348 Da, and peak molecular weights (Mp) of 2665 and 287 Da.

Amino acids contents and phytochemical characterization of CCPP and FCP

As shown in Table 3, FCP, as the main component of CCPP, contained a total of 17 amino acids, among which lysine, phenylalanine, methionine, threonine, isoleucine, leucine, valine, and histidine are essential amino acids, accounting for 8 of the 9 essential amino acids. In addition, glycine, phenylalanine, alanine, valine, leucine, isoleucine, proline, and methionine are hydrophobic amino acids. Glycine was the most abundant amino acid in FCP, followed by proline, glutamic acid, and alanine. The amino acid content of CCPP was relatively lower than that of FCP, but the composition was the same, with essential amino acids accounting for 37.06% of the total amino acid content. Glutamic acid was the most abundant amino acid in CCPP, followed by glycine, proline, and aspartic acid. The hydrophobic amino acids in CCPP included glycine, phenylalanine, alanine, valine, leucine, isoleucine, proline, and methionine, which accounted for 49.4% of the total amino acid content of CCPP. Quantification of the TPC and TFC was performed using standard curves with the formula

TABLE 1 Primer sequences.

Gene	Forward (5′–3′)	Reverse (5′–3′)
COL1A1	GAGGGCCAAGACGAAGACATC	CAGATCACGTCATCGCACAAC
COL1A2	GTTGCTGCTTGCAGTAACCTT	AGGGCCAAGTCCAACTCCTT
ELN	GCAGGAGTTAAGCCCAAGG	TGTAGGGCAGTCCATAGCCA
HAS2	CTCTTTTGGACTGTATGGTGCC	AGGGTAGGTTAGCCTTTTCACA
GAPDH	GGAGCGAGATCCCTCCAAAAT	GGCTGTTGTCATACTTCTCATGG

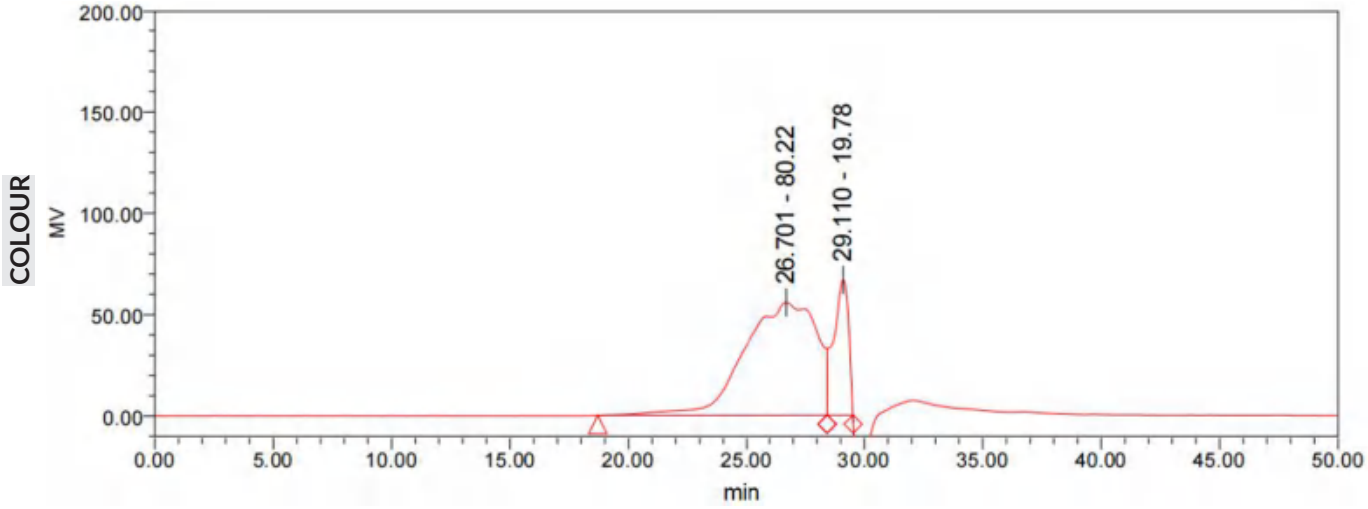

FIGURE 1 GPC chromatogram showing the CCPP molecular weight distribution.

TABLE 2 The results of molecular weight measured by GPC.

	Retention time (min)	Area (%)	Mn (Da)	Mw (Da)	Mz (Da)	Mp (Da)
1	26.701	80.22	2133	4696	11,289	2665
2	29.110	19.78	314	330	348	287

TABLE 3 The amino acid composition of CCPP and FCP.

Amino acid types	FCP (mg/g)	CCPP (mg/g)
Aspartic acid (Asp)	68.212	24.789
Threonine (Thr)	31.050	12.592
Serine (Ser)	47.409	10.827
Glutamic acid (Glu)	106.786	33.087
Glycine (Gly)	183.654	29.837
Alanine (Ala)	103.457	16.408
Cysteine (Cys)	28.608	3.098
Valine (Val)	33.290	10.751
Methionine (Met)	20.663	8.130
Isoleucine (Ile)	32.069	16.869
Leucine (Leu)	35.584	16.376
Tyrosine (Tyr)	13.678	7.919
Phenylalanine (Phe)	25.182	9.360
Histidine (His)	17.170	6.714
Lysine (Lys)	11.234	18.967
Argnine (Arg)	83.384	18.095
Proline (Pro)	134.156	25.353

Abs = aC + b generated by standard extracts of gallic acid (Figure 2A) and rutin (Figure 2B) at different concentrations. As shown in Figure 2C, the TPC of FCP was 1.81 ± 0.3 mg/g and the TFC was 0.21 ± 0.1 mg/g, while the TPC of CCPP was 15.20 ± 0.3 mg/g and the TFC was 4.7 ± 0.16 mg/g. The TPC and TFC of the collagen peptides significantly increased after the incorporation of acerola powder, broccoli powder, and cherry blossom powder ($p < 0.1$).

CCPP improved (UVA + UVB) induced skin photoaging in mice

First, we performed a simple in vivo study to verify the overall improvement in UVA + UVB-induced skin photoaging in mice provided by CCPP treatment. After UV irradiation, the mice showed more rough wrinkles on their backs and a leatherlike feel when touched (Figure 3A), while skin water content (Figure 3B) and oil content (Figure 3C) were significantly reduced ($p < 0.1$). HE staining showed that the epidermal layer was significantly thickened, the epidermal protrusions and dermal papillae were significantly reduced, and the epidermal–dermal junction tended to be flattened in the UV group mice compared with those in the Control group (Figure 3D). All of the above phenomena suggested that the UVA + UVB irradiation successfully replicated the mouse skin photoaging model.[30] Mice in the CCPP and FCP groups showed a significant reduction in skin wrinkles and their back skins felt more similar to the Control group (Figure 3A), while the skin water content (Figure 3D) and oil content

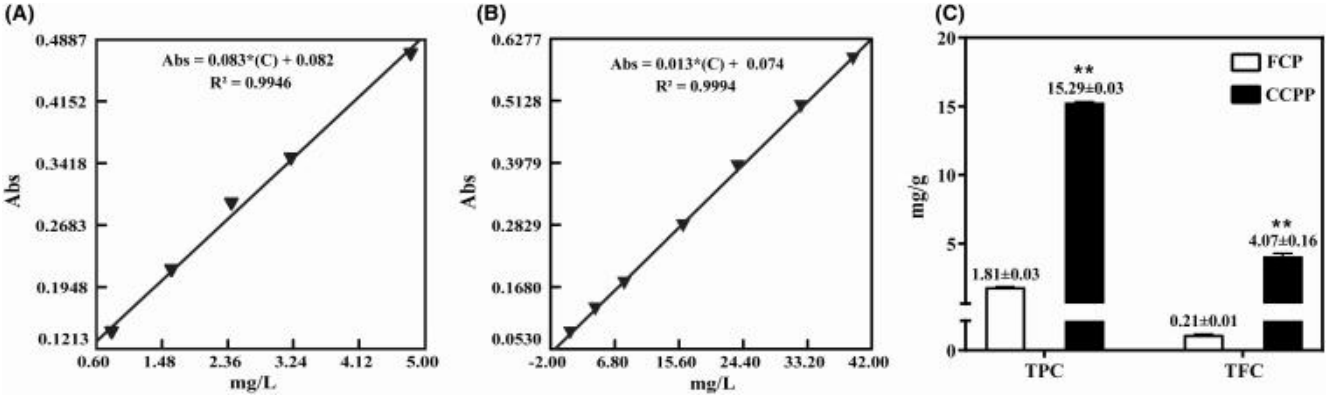

FIGURE 2 Determination of TPC and TFC. (A) The calibration line was constructed by plotting the absorbance that corresponded to different concentrations of gallic acid. (B) The calibration line was constructed by plotting the absorbance that corresponded to different concentrations of rutin. Abs, absorbance; C, concentration. (C) Comparison of TPC, and TFC between CCPP and FCP. Data are presented as the mean ± SD ($n = 3$). *$p < 0.05$ and **$p < 0.01$ compared to the FCP group.

COLOUR

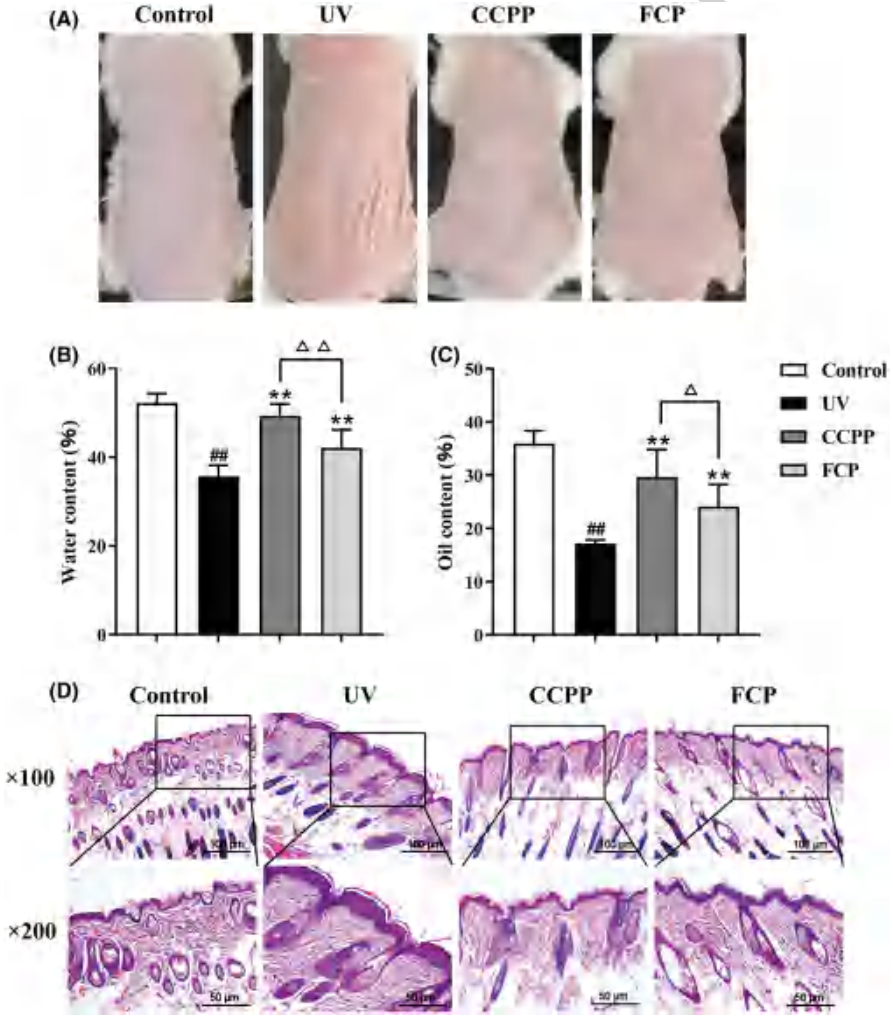

FIGURE 3 Effect of CCPP on (UVA + UVB) induced skin photoaging in mice. (A) Images of the skins of mice 24 h after the last treatment. (B) Skin water content. (C) Skin oil content. (D) HE staining images of skin tissue (magnification: 100×, scale bar: 100 μm; magnification: 200×, scale bar: 50 μm). Data are presented as the mean ± SD ($n = 10$). $^{\#}p < 0.05$ and $^{\#\#}p < 0.01$ compared to the Control group; *$p < 0.05$ and **$p < 0.01$ compared to the UV group; $^{\triangle}p < 0.05$ and $^{\triangle\triangle}p < 0.01$ comparing the CCPP M and FCP groups.

(Figure 3C) were significantly higher ($p < 0.1$). HE staining also showed significant thinning of the epidermal layer, an increase in the number of epidermal protrusions and dermal papillae, and wavy undulations at the epidermal–dermal junction in the CCPP and FCP groups of mice (Figure 3D). Moreover, we compared the CCPP group with the FCP group and found that the CCPP group mice had fewer skin wrinkles, and the skin appearance, as well as the feel, was similar to the Control group (Figure 3A). Additionally, the skin water content (Figure 3B) and oil content (Figure 3C) were significantly higher than those of the FCP group ($p < 0.5$). The HE staining images showed a thinner epidermal layer and more epidermal protrusions in the CCPP group (Figure 3D). In conclusion, both orally administered CCPP and FCP were effective in improving skin photoaging by reducing skin wrinkles, increasing skin water and oil contents, and restoring skin histopathological changes. The CCPP exhibited superior overall improvement compared to FCP at an equivalent dosage.

CCPP restored cell viability and promoted cell proliferation

UVA was used to generate a human skin fibroblast BJ cell photoaging model.[31] Cell viability decreased in a dose-dependent manner under different doses of UVA irradiation, with a significant decrease in cell viability at $>10\,J\,cm^{-2}$ compared to that in the Control group. Moreover, BJ cell viability under $30\,J\,cm^{-2}$ UVA irradiation was close to half that in the Control group (Figure 4A). Therefore, this dose was used for inducing cell photoaging in subsequent experiments.[28] BJ cell viability was significantly lower in the 25 mg/mL CCPP treatment group than in the control group ($p < 0.001$), indicating that CCPP is toxic to BJ cells at this dose. However, CCPP at a concentration of <25.00 mg/mL did not have a significant toxic effect on BJ cells (Figure 4B). Therefore, in this study, 3.13 mg/mL, 6.25 mg/mL, and 12.50 mg/mL were selected as the low, medium, and high treatment concentrations of CCPP, respectively. Moreover, a significant decrease in BJ cell viability was observed at an FCP concentration of 50.00 mg/mL ($p < 0.005$), indicating that FCP was toxic to these cells at this dose. Conversely, FCP at a concentration of <50.00 mg/mL did not have a significant toxic effect on BJ cells (Figure 4C). Consequently, we selected 6.25 mg/mL as the sole in vitro treatment concentration of FCP and compared the acquired data with those obtained at the same treatment concentration of CCPP (medium concentration of CCPP, 6.25 mg/mL). The viability and number of $Ki67^+$ (a reliable intranuclear marker of cell proliferation) BJ cells decreased significantly after UVA irradiation ($p < 0.001$). After treatment with CCPP and FCP, cell viability was markedly elevated in comparison with that in the UVA group ($p < 0.005$), while the cell viability in the CCPP M group was significantly greater than that in the FCP group ($p < 0.005$) (Figure 4D). Furthermore, the proportions of $Ki67^+$ cells were dramatically greater in the CCPP H and CCPP M groups than in the UVA group ($p < 0.005$), and the difference between the CCPP M group and the FCP group was notable ($p < 0.005$) (Figure 4E,F). These results implied that CCPP could restore cell viability and promote cell proliferation and that an equivalent treatment concentration of FCP had a weaker effect than CCPP.

CCPP reduced the extent of UVA-induced cellular senescence

The alterations in cellular morphology are depicted in Figure 5A. Following UVA irradiation, a reduction in cell count was observed, accompanied by cytoplasmic shrinkage and indistinct cell margins, consistent with the phenotypic changes associated with senescence in human skin fibroblasts.[28] The CCPP treated and FCP groups exhibited a higher proportion of cells displaying distinct morphology, more organized arrangement, and morphology resembling that of the Control group. SA β gal staining is a representative method to assess the level of cellular senescence, and the extent of SA β gal staining in cells is positively correlated with the degree of cellular senescence.[29] After UVA irradiation, the percentage of SA β gal positive cells (Figure 5B,C) was significantly increased ($p < 0.001$), and the cells showed accelerated senescence. After CCPP and FCP treatment, the percentages of SA β gal positive cells (Figure 5B,C) were significantly reduced ($p < 0.001$). Moreover, the percentage of SA β gal positive cells in the CCPP M group (Figure 5B,C) was significantly lower than that in the FCP group ($p < 0.005$). The above results indicated that both CCPP and FCP were able to reduce UVA induced photoaging of human skin fibroblasts, and the effect of CCPP was better than that of FCP at the same dose.

CCPP reduced UVA induced intracellular ROS levels and attenuated oxidative stress

After exposure to UVA irradiation, the mean fluorescence intensity of intracellular ROS (Figure 6A,B) was significantly increased ($p < 0.001$), indicating that UVA irradiation significantly elevated the ROS level in the cells. However, the ROS levels in the cells in the CCPP H, CCPP M, and FCP groups (Figure 6A,B) were significantly lower ($p < 0.005$). The levels of the antioxidant

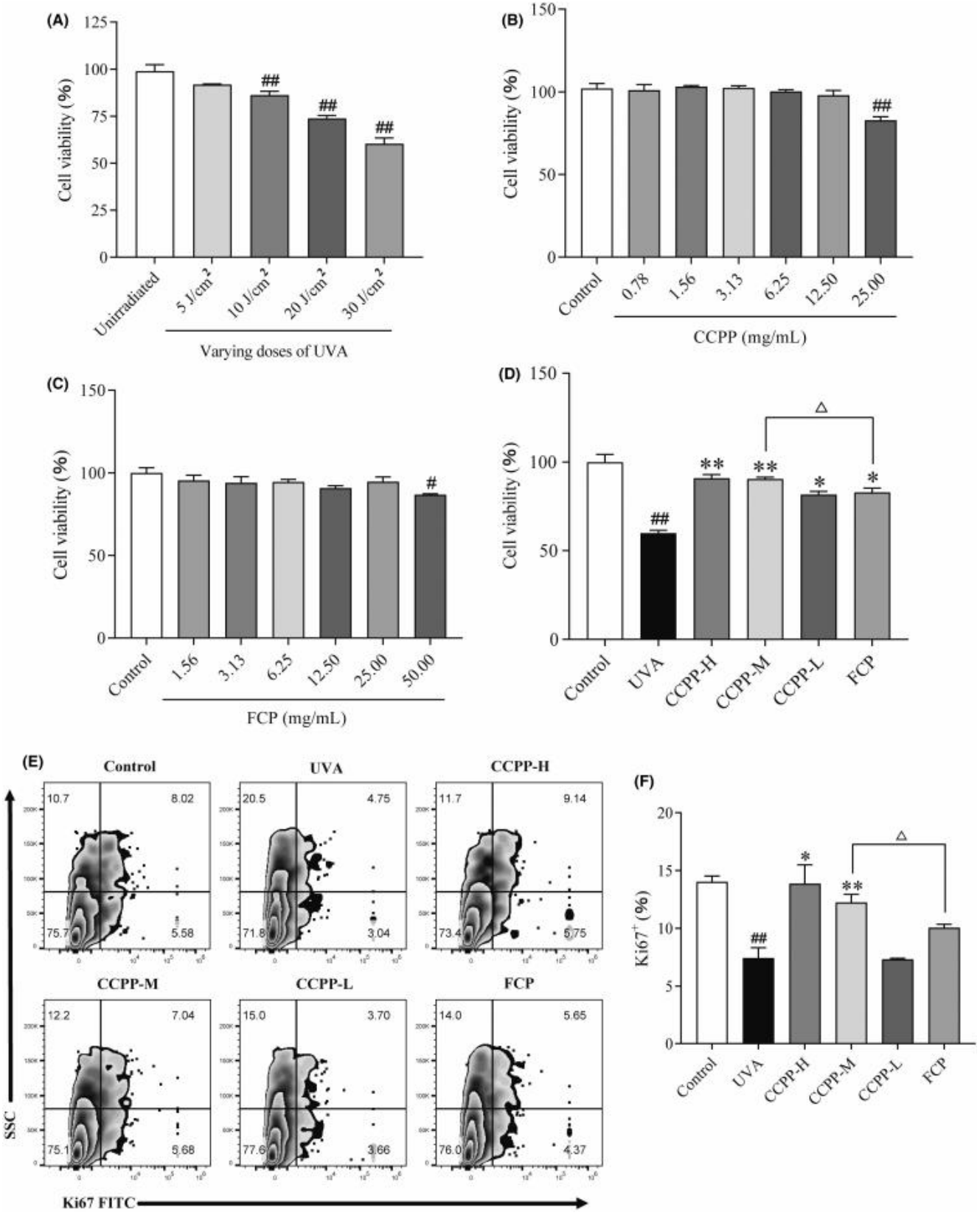

FIGURE 4 Effect of CCPP on the viability of BJ cells with or without UVA irradiation. (A) Cell viability at different UVA irradiation doses. (B) Cell viability at different CCPP treatment concentrations. (C) Cell viability at different FCP treatment concentrations. (D) Effect of CCPP and FCP on cell viability after UVA treatment. (e f) Ki67$^+$ BJ cells analysis. Data are presented as the mean ± SD ($n = 3$–5). $^{\#}p < 0.05$ and $^{\#\#}p < 0.01$ compared to the Control group; $^{*}p < 0.05$ and $^{**}p < 0.01$ compared to the UVA group; $^{\triangle}p < 0.05$ and $^{\triangle\triangle}p < 0.01$ comparing the CCPP M and FCP groups.

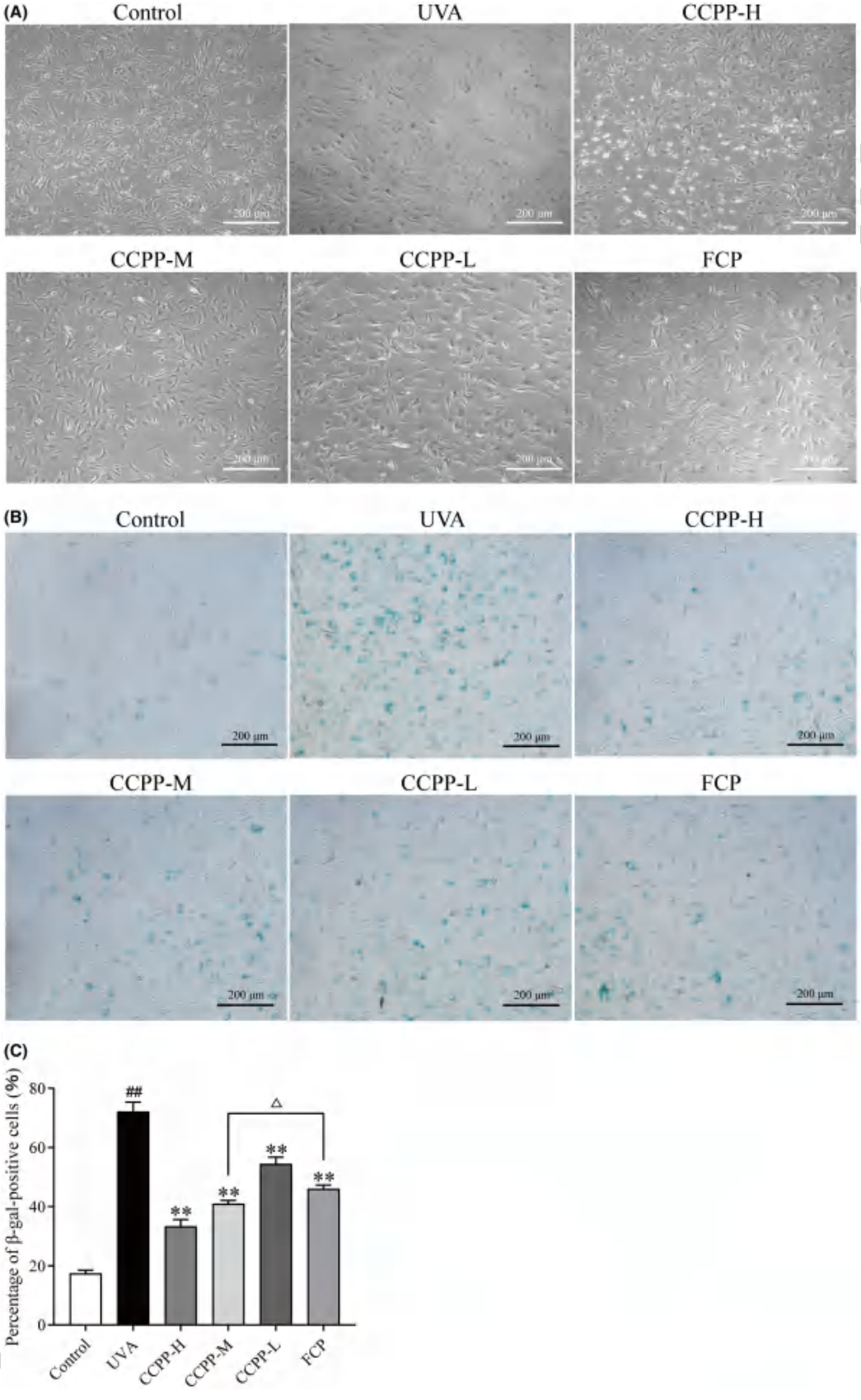

COLOUR

FIGURE 5 Effect of CCPP on the morphology of and SA β gal levels in BJ cells after UVA irradiation. (A) Changes in cell morphology (magnification: 50×, scale bar: 200 μm). (B) SA β gal staining images (magnification: 50×, scale bar: 200 μm). (C) Number of SA β gal positive cells as a percentage of total cells. Data are presented as the mean ± SD ($n = 5$). $^{\#}p < 0.05$ and $^{\#\#}p < 0.01$ compared to the Control group; $^{*}p < 0.05$ and $^{**}p < 0.01$ compared to the UVA group; $^{\triangle}p < 0.05$ and $^{\triangle\triangle}p < 0.01$ comparing the CCPP M and FCP groups.

6

COLOUR

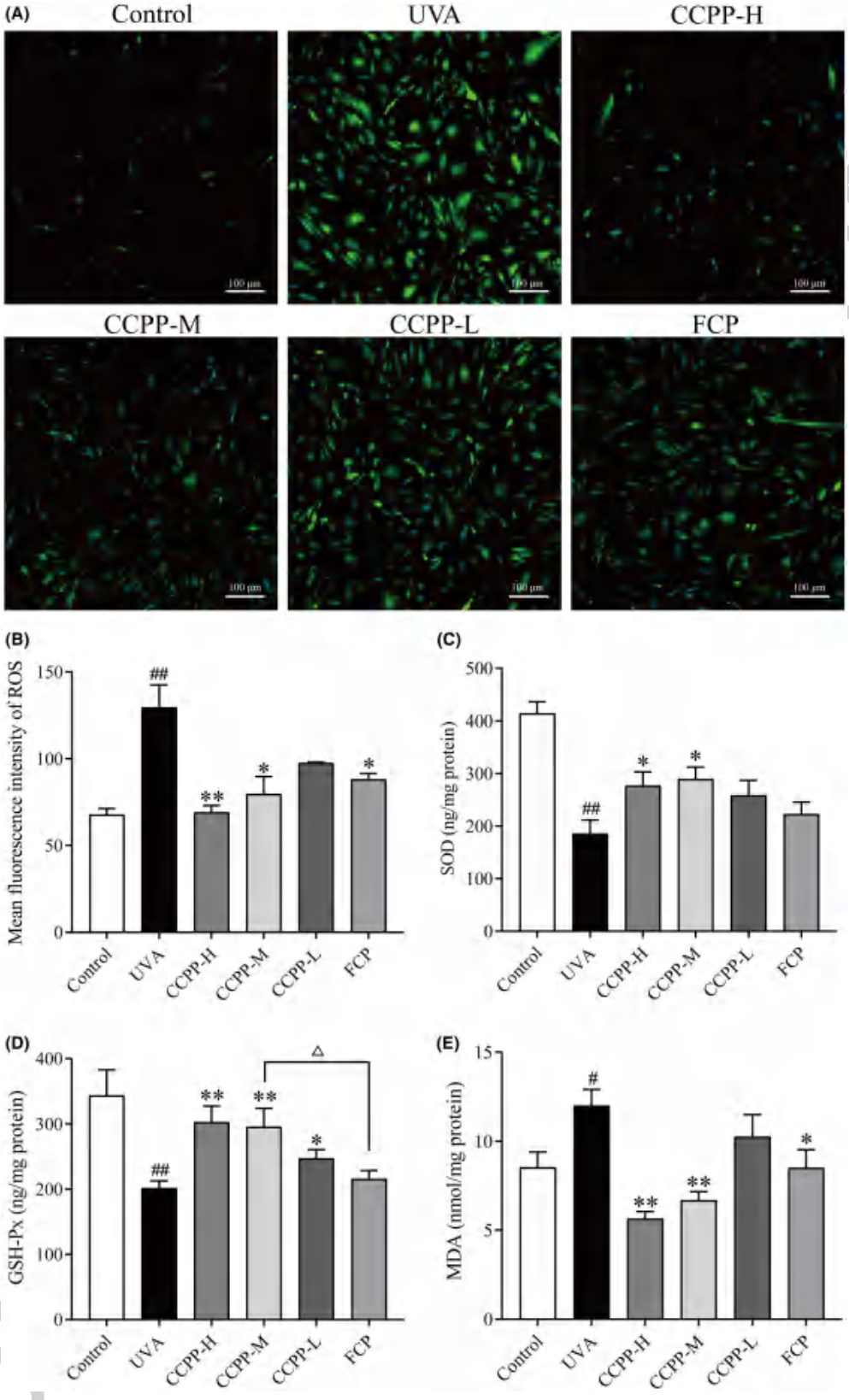

FIGURE 6 Effect of compound collagen peptide powder on the levels of ROS, SOD, GSH Px, and MDA in BJ cells after UVA irradiation. (A) The fluorescent probe DCFH DA was used to detect intracellular ROS levels (magnification: 100×, scale bar: 100 μm). (B) Mean fluorescence intensity of ROS analyzed by ImagePro Plus 6.0 software. (C) Intracellular SOD levels measured by ELISA. (D) Intracellular GSH Px levels measured by ELISA. (E) Intracellular MDA levels measured by ELISA. Data are presented as the mean ± SD ($n = 3–5$). $^{\#}p < 0.05$ and $^{\#\#}p < 0.01$ comp red to the Control group; $^{*}p < 0.05$ and $^{**}p < 0.01$ compared to the UVA group; $^{\triangle}p < 0.05$ and $^{\triangle\triangle}p < 0.01$ comparing the CCPP M and FCP groups.

enzymes SOD and GSH Px and the cell membrane lipid peroxidation product MDA can reflect the extent of oxidative stress damage.[32] After exposure to UVA irradiation, the levels of SOD and GSH Px in cells (Figure 6C,D) were significantly diminished ($p < 0.001$), and the level of MDA (Figure 6E) was markedly elevated ($p < 0.005$). These findings suggested an exacerbation of cellular oxidative stress damage following UVA irradiation. Importantly, the levels of SOD (Figure 6C) (except for the CCPP L group) and GSH Px (Figure 6D) were significantly higher in the CCPP-treated groups ($p < 0.005$), while MDA levels (Figure 6E) were significantly lower in the CCPP H, CCPP M, and FCP groups ($p < 0.005$). The GSH Px levels in the CCPP M group (Figure 6D) were significantly elevated compared to those observed in the FCP group ($p < 0.005$). In conclusion, CCPP and FCP could significantly reduce UVA-induced oxidative stress in human skin fibroblasts, and the antioxidant effect of CCPP was superior to that of FCP at the same dose.

CCPP increased ECM synthesis in human skin fibroblasts

COL1, ELN, and HA are produced by skin fibroblasts, which are important to the ECM in the dermis and are key indicators for assessing the effectiveness of functional foods for skin supplementation.[33] COL1 consists of two identical collagen type 1 α1 chain (COL1A1) and one collagen type 1 α2 chain (COL1A2); hyaluronan synthase 2 (HAS2) is a major player in HA biosynthesis.[34] In the present study, the expression levels of COL1, *COL1A1* mRNA, *COL1A2* mRNA, ELN, *ELN* mRNA, HA, and *HAS2* mRNA (Figure 7A–G) in human skin fibroblasts after UVA irradiation were significantly reduced ($p < 0.005$), indicating that the ECM synthesis function in BJ cells was diminished. The expression levels of COL1 (except for the CCPP L group), *COL1A1* mRNA (except for the CCPP L group), *COL1A2* mRNA, ELN (except for the CCPPL group), *ELN* mRNA (except in the CCPP L group), HA (except for the CCPP L and FCP groups), and *HAS2* mRNA (except in the CCPP L group) were significantly increased in both the CCPP and FCP treated groups (Figure 7A–G) ($p < 0.005$). Moreover, the expression levels of COL1 (Figure 7A), *COL1A2* mRNA (Figure 7C), and *HAS2* mRNA (Figure 7G) in the CCPP M group were significantly higher than those in the FCP group ($p < 0.005$). In conclusion, both CCPP and FCP significantly enhanced ECM synthesis in UVA-irradiated human skin fibroblasts, with the effect of CCPP being more pronounced than that of FCP at the same treatment concentration.

CCPP promoted human skin fibroblast proliferation and ECM synthesis through activation of the TGF β1/Smad pathway

The TGF β1/Smad pathway is a classical signaling pathway that modulates a variety of cellular processes, including ECM synthesis and cell proliferation.[35] To identify effective pathways by which CCPP mediates the synthesis of ECM and promotes proliferation in BJ cells, we employed Western blot to detect the expression of upstream, core, and downstream proteins in the TGF β1/Smad pathway. The protein expression levels of TGF β1, TGF βR2, Smad2, Smad3, and Smad2/3 (Figure 8A–F) in UVA irradiated human skin fibroblasts were significantly downregulated ($p < 0.005$), indicating attenuation of the TGF β1/Smad signaling pathway in response to UVA irradiation treatment. The protein expression levels of TGF β1, TGF βR2 (except for the CCPP L and FCP groups), Smad2, Smad3, and Smad2/3 were significantly upregulated following treatment with CCPP and FCP ($p < 0.005$). This observation demonstrated the ability of both CCPP and FCP to enhance TGF β1/Smad signaling in photoaged human skin fibroblasts. To further investigate whether CCPP promotes human skin fibroblast proliferation and mediates ECM synthesis through activation of the TGF β1/Smad pathway, some cells were pretreated with the TGF β receptor inhibitor LY2109761 (5 μM) for 2 h before treatment.[36] After LY2109761 pretreatment of normal BJ cells for 2 h, TGF βR2 and Smad2/3 protein expression levels (Figure 8G,H) were significantly reduced ($p < 0.001$), demonstrating that the conditions used by LY2109761 to block the TGF β1/Smad pathway were stable. The percentage of $Ki67^+$ cells (Figure 8I,J) in the CCPP H + LY2109761 group was significantly decreased compared to that in the CCPP H group ($p < 0.001$), indicating that the proliferation-promoting effect of CCPP on photoaged human skin fibroblasts was completely blocked after pretreatment with LY2109761. Similarly, COL1 (Figure 8K), ELN (Figure 8I), and HA (Figure 8M) levels were significantly decreased in the CCPP H + LY2109761 group compared with the CCPP H group ($p < 0.005$), indicating that the CCPP mediated promotion of ECM synthesis was completely blocked after pretreatment with LY2109761. Thus, blockade of the TGF β1/Smad signaling pathway counteracted the promotion of human skin fibroblast proliferation and ECM synthesis by CCPP treatment. All the aforementioned experimental results indicated that CCPP facilitated the proliferation and ECM synthesis in human skin fibroblasts by activating the TGF β1/Smad signaling pathway.

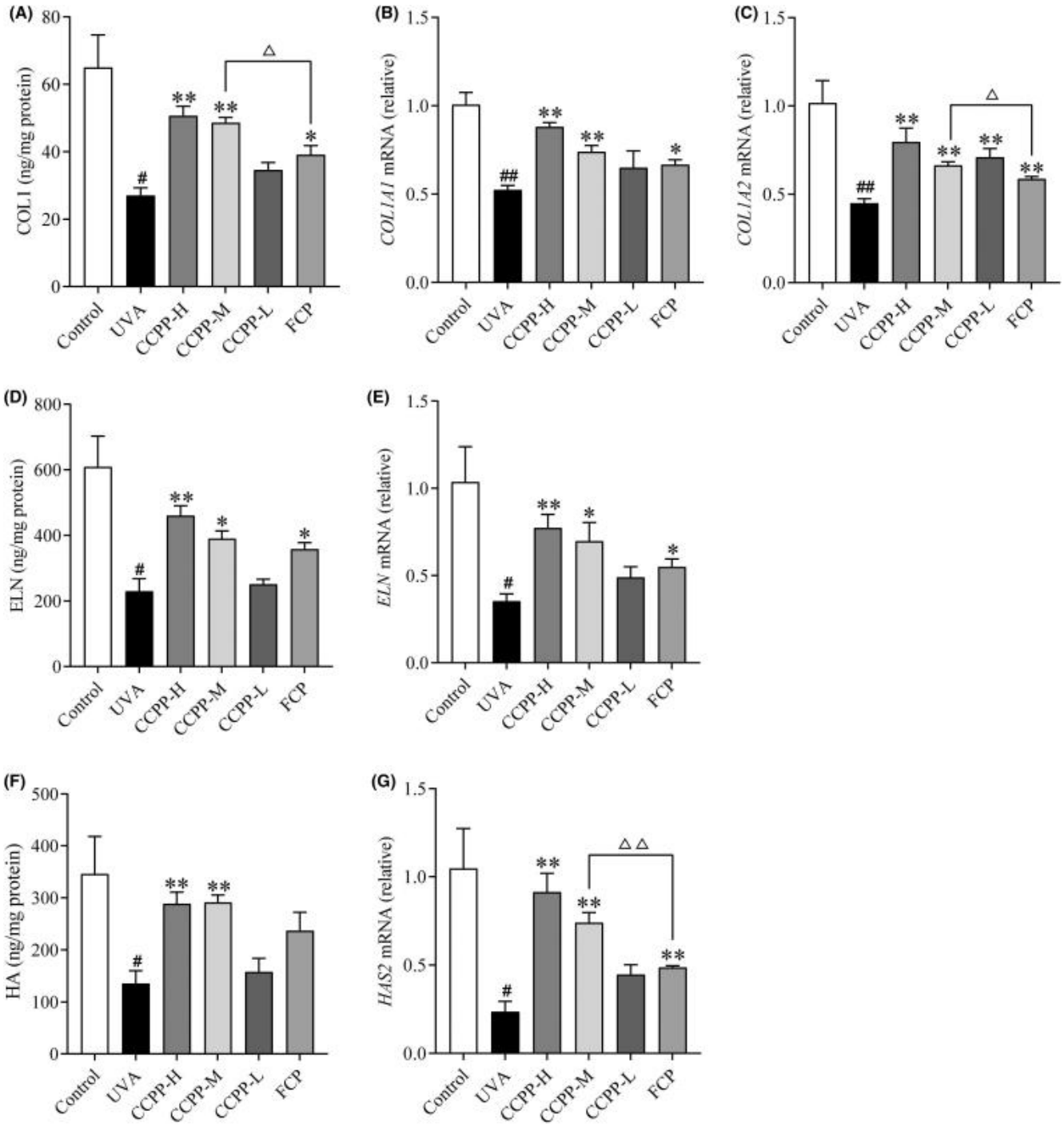

FIGURE 7 Effect of CCPP on ECM synthesis in UVA irradiated BJ cells. (A) COL1 levels were measured by ELISA. (B) *COL1A1* mRNA levels measured by qPCR. (C) *COL1A2* mRNA levels measured by qPCR. (D) ELN levels measured by ELISA. (E) *ELN* mRNA levels measured by qPCR. (F) HA levels measured by ELISA. (G) *HAS2* mRNA levels measured by qPCR. Data are presented as the mean ± SD ($n = 3$). $^{\#}p < 0.05$ and $^{\#\#}p < 0.01$ compared to the Control group; $^{*}p < 0.05$ and $^{**}p < 0.01$ compared to the UVA group; $^{\triangle}p < 0.05$ and $^{\triangle\triangle}p < 0.01$ comparing the CCPP M and FCP groups.

DISCUSSION

Currently, the majority of studies have focused primarily on evaluating the efficacy and investigating the underlying mechanisms of individual components with potential antiphotoaging properties. However, the efficacy and bioavailability of such individual components are limited. To combat these problems, researchers are increasingly turning to antiphotoaging studies with multi ingredient complexes. Multi ingredient complexes can synergistically incorporate diverse antiphotoaging ingredients to enhance efficacy while facilitating improved

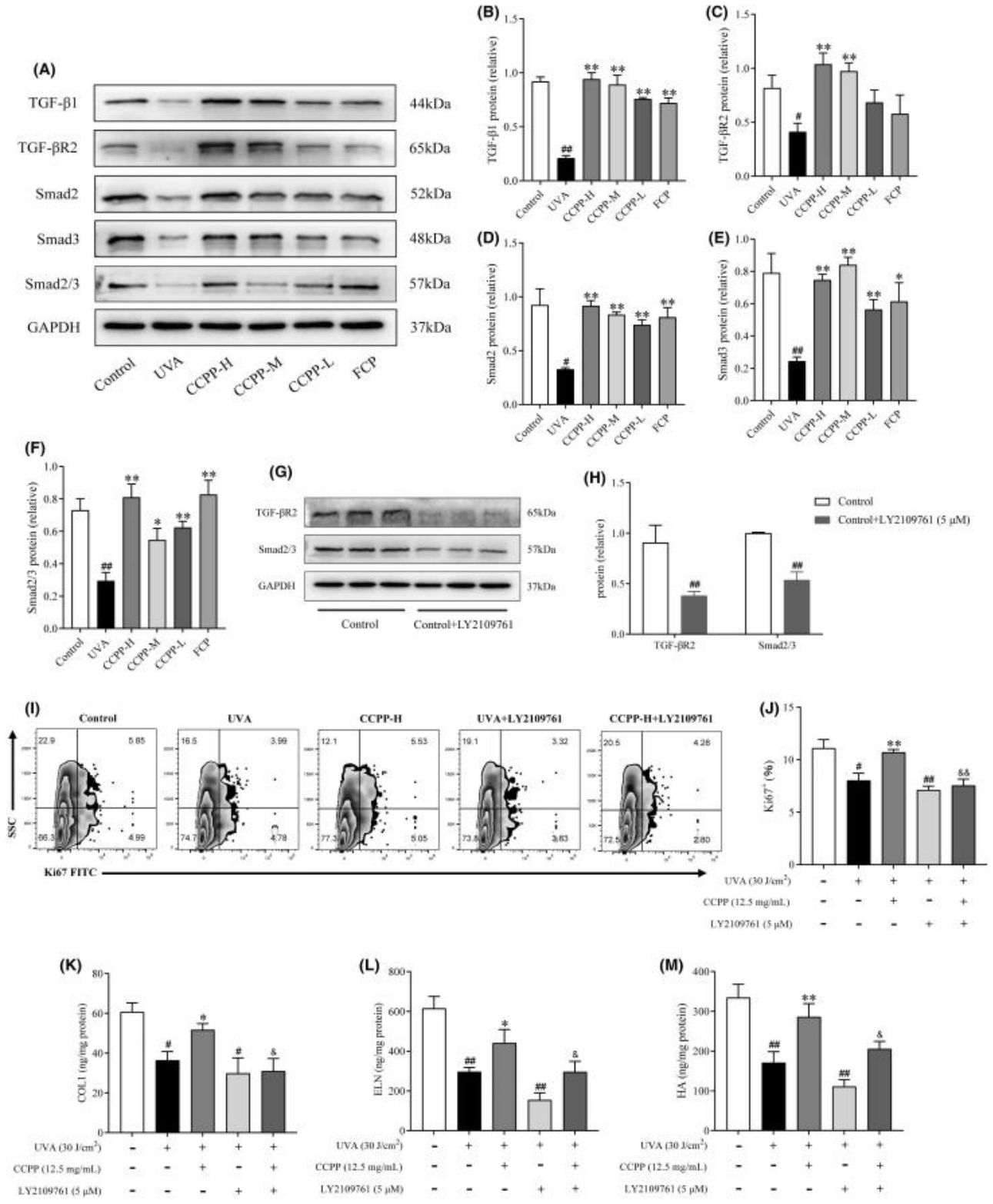

FIGURE 8 Effect of CCPP on the TGF β1/Smad signaling pathway in UVA irradiated BJ cells. (A) The protein expression of TGF β1, TGF βR2, Smad2, Smad3, and Smad2/3 in BJ cells was analyzed by Western blotting; GAPDH served as a reference for all proteins. (B–F) Quantitative evaluations of TGF β1, TGF βR2, Smad2, Smad3, and Smad2/3 protein levels by determination of the strip grayscale values by ImagePro Plus 6.0 software. (G) Western blotting was used to analyze the effect of LY2109761 pretreatment on TGF βR2 and Smad2/3 protein expression in normal BJ cells. (H) Quantitative evaluations of TGF βR2 and Smad2/3 protein levels. (I\J) $Ki67^+$ BJ cells analysis. (K) COL1 levels were measured by ELISA. (L) ELN levels measured by ELISA. (M) HA levels measured by ELISA. Data are presented as the mean ± SD ($n = 3$). $^{\#}p < 0.05$ and $^{\#\#}p < 0.01$ compared to the Control group; $^{*}p < 0.05$ and $^{**}p < 0.01$ compared to the UVA group; $^{\triangle}p < 0.05$ and $^{\triangle\triangle}p < 0.01$ comparing the CCPP M and FCP groups; $^{\&}p < 0.05$ and $^{\&\&}p < 0.01$ compared to the CCPP H group.

bioavailability and stability through intermolecular interactions. For example, natural plant ingredients are incorporated into foods to impart the food with certain phytochemical properties. Cinnamon powder is added to bread to increase the contents of polyphenols, flavonoids, and condensed tannins, and the antioxidant properties are proportional to the proportion of cinnamon powder added.[37] The incorporation of different ratios of quinoa flour into wheat flour during cookie production resulted in a significant increase in the phenolic and flavonoid contents of the cookies, which also showed a favorable hypoglycemic effect.[38] In our investigation, CCPP was prepared by incorporating appropriate proportions of acerola powder, broccoli powder, and cherry blossom powder into FCP. The small molecular weight of CCPP suggested its high bioavailability, facilitating its rapid absorption by the body and efficient distribution to various tissues via systemic circulation, thereby exerting nourishing and reparative effects.[39] Chemical composition analysis revealed that CCPP contained a markedly elevated TPC and TFC, which are associated with phytochemical properties and enhanced antioxidant potential.[40] In addition, the bioactivity of collagen peptides depends considerably on their amino acid composition.[41] Glycine, proline, and glutamic acid are the major amino acids in collagen hydrolysates, and are beneficial for skin water retention and wound healing.[42,43] Moreover, some antioxidant active peptides isolated from protein hydrolysates contain hydrophobic amino acids at both the C terminal and N terminal ends, and a higher content of hydrophobic amino acids indicates certain dominance of antioxidant properties.[44] As the major raw material of CCPP, FCP contains 8 essential amino acids and 8 hydrophobic amino acids, with glycine, proline, and glutamic acid collectively constituting 43.5% of the total amino acid content, while hydrophobic amino acids account for 58.2%. The unique amino acid composition of FCP conferred CCPP with its unexpected nutritional properties and antioxidant potential.

With the weakening of the protective effect provided by the ozone layer and the increase in the number of people working outdoors, the effects of UV are hard to ignore, and skin photoaging has become a danger to people that cannot be underestimated. External symptoms of skin photoaging are usually characterized by dry and rough skin, hyperkeratosis, sagging, inelasticity, visible wrinkles, and pigmentation,[45] which greatly reduce the quality of life. Most of the UV in sunlight that reaches the surface of the earth is in the form of UVA and UVB rays. To most closely simulate the change process of photoaging in organisms, we first used UVA + UVB to establish an in vitro model of skin photoaging in mice.[46] After 9 weeks of UV irradiation, the dorsal skins of the mice showed significant wrinkles and a significant decrease in both skin water content and oil content. These macroscopic lesions may be due to a large loss of ECM within the dermis and a decrease in sebaceous gland secretion.[33] The administration of CCPP orally effectively reversed skin wrinkles, skin water, and oil content, as well as histopathological changes in photoaged mice. Our in vivo study first demonstrated that oral administration of CCPP was effective in ameliorating the symptoms of skin photoaging in mice.

We subsequently further determined the anti-photoaging property of CCPP and the specific mechanism of action by in vitro cellular experiments. Only a few UVB rays can reach the dermis, as most are absorbed by the epidermis, while UVA can reach the dermis directly, and fibroblasts are the most abundant cells in the dermis.[47] Hence, UVA radiation was employed to establish an in vitro model of human skin fibroblast photoaging. The CCPP treatment effectively restored cellular morphology, significantly enhanced cell viability, and substantially increased cell numbers. Moreover, the SA β gal level in the cells was significantly reduced by CCPP. These results suggested that CCPP can inhibit the photoaging process of human skin fibroblasts, which was consistent with our in vivo experimental results. It is worth noting that UVB, due to its higher energy, can more rapidly inflame the epidermis and cause DNA damage.[48] The effect of UVB on keratinocytes is highly correlated with the thickening of the epidermis that has been observed in pathological sections of skin from photoaged mice.[49] Although this study was conducted in fibroblasts, it would be intriguing for us to investigate the potential beneficial effects of CCPP on keratinocytes in future studies.

Previous studies have shown that exposure of organisms and skin cells to high-intensity UV irradiation or for long periods of time makes them highly susceptible to the production and excessive accumulation of ROS.[50,51] Importantly, ROS can induce oxidative stress in tissues and cells, degrade various antioxidant enzymes, and promote lipid peroxidation and protein, lipid, or nucleic acid glycosylation, thus continuously aggravating oxidative damage.[52] Moreover, ROS can increase the transcriptional activity of activator protein 1 (AP 1) by activating the mitogen-activated protein kinase (MAPK) signaling cascade, which induces the expression of matrix metalloproteinases (MMPs),[53] the main cause of collagen degradation in the skin. Additionally, AP 1 also reduces ECM synthesis by inhibiting the TGF β1/Smad pathway,[54] indirectly leading to the loss of nutrients from the dermis. In this study, CCPP treatment was able to significantly reduce the level of ROS in cells, elevate the levels of SOD and GSH Px, and reduce MDA production. This result indicated that CCPP could enhance the antioxidant capacity of human skin fibroblasts and attenuate oxidative damage.

We have shown that UVA irradiation reduced the levels of COL1, ELN, HA, and HAS2 and the expression of

the corresponding genes in human skin fibroblasts. COL1 and ELN are structural proteins that play a supportive, filling role and are essential for maintaining the fullness and elasticity of the skin.[55] The ability of CCPP to increase COL1 and ELN levels and the expression of the corresponding genes in fibroblasts was consistent with the fact that CCPP significantly reduced wrinkles on the skin of photoaged mice. HA is the "moisturizing factor" in the skin, acting as a nourishing agent and determining the moisturizing capacity of the skin.[56] Hyaluronate synthase (HAS) synthesizes HA in the cell membrane, with HAS2 being the most important isoform of HAS with the highest expression.[2] In this study, CCPP was able to elevate HA levels in fibroblasts while upregulating *HAS2* mRNA expression, which seemed to have a significant association with the CCPP-mediated elevation in skin water content in mice in vivo. Furthermore, unexpected findings have demonstrated that the degradation of collagen yields collagen fragments capable of activating αvβ3 integrin signaling, thereby resulting in a downregulation of HAS2 expression.[57] These findings provide crucial insights for our subsequent investigations into the potential regulatory role of CCPP in αvβ3 integrin signaling or the development of functional foods that modulate αvβ3 integrin signaling.

TGF β1 is a cytokine that plays important roles in cell growth, differentiation, and ECM synthesis, and its downstream proteins Smad2, Smad3, and Smad4 are responsible for intracellular to nuclear signaling.[58] TGF β1 binds to its cell membrane receptors, TGF βR1 and TGF βR2, initiating the revitalization of Smad2 and Smad3 proteins. Subsequently, the activated Smad2/3 protein forms a heterodimeric complex with Smad4 and translocates to the nucleus. This complex activates relevant promoters and facilitates ECM expression.[35] It has been reported that the TGF β1/Smad pathway is positively correlated with the ECM levels in skin tissues, and is associated with the proliferation and apoptosis process of skin cells.[9] Currently, it has been shown that influencing ECM synthesis by modulating TGF β1/Smad signaling can positively affect skin tissues and cells under UV irradiation. Chlorogenic acid,[4] Santamarine,[59] and Corn silk extract[60] are known to mitigate skin photoaging by increasing collagen fiber deposition through activation of the TGF β1/Smad pathway. In the present study, we found that CCPP-activated TGF β1/Smad signaling, which led us to hypothesize that the pathway that promotes proliferation and ECM synthesis in human skin fibroblasts involves at least the TGF β1/Smad pathway. To provide convincing evidence, an inhibitor of the classical TGF β receptor was used to block TGF β1/Smad signaling, and it was found that the promotion of COL1, ELN, and HA synthesis and cell proliferation by CCPP diminished. These experimental results enabled us to determine that the TGF β1/Smad signaling pathway mediates the process of ECM synthesis and cell proliferation in human skin fibroblasts.

In summary, CCPP can effectively ameliorate skin photoaging in mice, inhibit the aging of human skin fibroblasts, significantly reduce the oxidative stress response, and increase ECM synthesis in vitro. By comparing its efficacy with that of the FCP group, CCPP demonstrated a more significant effect on skin photoaging, suggesting that the incorporation of acerola powder, broccoli powder, and cherry blossom powder contributed to enhancing the antiphotoaging function of the collagen peptide. This study provides an innovative idea and theoretical basis for the further advancement and application of composite collagen peptide-like functional foods, giving novel insights into strategies to improve skin photoaging. Notably, our investigation focused solely on one formulation with a specific component ratio and did not comparatively evaluate the properties exhibited by each individual component present in varying ratios. Therefore, in addition to continuously exploring potential food additives with photoprotective properties, our next study will also focus on determining the optimal ratio of each component.

AUTHOR CONTRIBUTIONS

Kaien Guo: Methodology, Investigation, Formal analysis, Writing; Linxin Zheng: Resources, Data curation, Visualization; Xin Zeng: Supervision, Project administration; Guangchun Huang: Investigation; Lingling Meng: Investigation; Yuting Yin: Supervision, Project administration, Funding acquisition.

ACKNOWLEDGMENTS

The authors thank Jiangxi Wufang Biotechnology Co., Ltd for supplying all the materials and Jiangxi University of Chinese Medicine for providing the experimental platform.

FUNDING INFORMATION

This study was supported by the Jiangxi Provincial Chinese Medicine Young and Middle-aged Backbone Talents (Fourth Batch) Training Program Project, Jiangxi University of Chinese Medicine Science and Technology Innovation Team Development Program (No. CXTD22007), and Jiangxi College Students' Innovation and Entrepreneurship Training Program Project (No. S202310412063).

CONFLICT OF INTEREST STATEMENT

The authors declare no conflicts of interest.

DATA AVAILABILITY STATEMENT

Relevant data included in the results of this study are available from the corresponding author upon request.

ORCID

Kaien Guo https://orcid.org/0000-0002-4266-6033

REFERENCES

1. Choi SI, Han HS, Kim JM, et al. Eisenia bicyclis extract repairs UVB induced skin Photoaging in vitro and in vivo: Photoprotective effects. *Mar Drugs*. 2021;19:693.
2. Kang MK, Kim DY, Oh H, et al. Dietary collagen hydrolysates ameliorate furrowed and parched skin caused by Photoaging in hairless mice. *Int J Mol Sci*. 2021;22:6137.
3. Deng M, Yu TZ, Li D, et al. Human umbilical cord mesenchymal stem zcell-derived and dermal fibroblast derived extracellular vesicles protect dermal fibroblasts from ultraviolet radiation induced photoaging in vitro. *Photochem Photobiol Sci*. 2020;19:406-414.
4. Xue N, Liu Y, Jin J, Ji M, Chen X. Chlorogenic acid prevents UVA induced skin Photoaging through regulating collagen metabolism and apoptosis in human dermal fibroblasts. *Int J Mol Sci*. 2022;23:6941.
5. Xu P, Xin Y, Zhang Z, et al. Extracellular vesicles from adipose derived stem cells ameliorate ultraviolet B induced skin photoaging by attenuating reactive oxygen species production and inflammation. *Stem Cell Res Ther*. 2020;11:264.
6. Lee SJ, Kim JE, Choi YJ, et al. Antioxidative role of Hygrophila erecta (Brum. F.) Hochr. On UV induced Photoaging of dermal fibroblasts and melanoma cells. *Antioxidants (Basel)*. 2022a;11:1317.
7. Chen H, Li Y, Xie X, et al. Exploration of the molecular mechanisms underlying the anti Photoaging effect of *Limosilactobacillus fermentum* XJC60. *Front Cell Infect Microbiol*. 2022;12:838060.
8. Yang F, Hyun J, Nagahawatta DP, Kim YM, Heo MS, Jeon YJ. Cosmeceutical effects of Ishige Okamura Celluclast extract. *Antioxidants (Basel)*. 2022;11:2442.
9. Fu Y, Li C, Wang Q, et al. The protective effect of collagen peptides from bigeye tuna (*Thunnus obesus*) skin and bone to attenuate UVB induced photoaging via MAPK and TGF β signaling pathways. *J Funct Foods*. 2022;93:105101.
10. Lee M, Kim D, Park SH, et al. Fish collagen peptide (Naticol(®)) protects the skin from dryness, wrinkle formation, and Melanogenesis both in vitro and in vivo. *Prev Nutr Food Sci*. 2022b;27:423-435.
11. Bocheva G, Slominski RM, Slominski AT. The impact of vitamin D on skin aging. *Int J Mol Sci*. 2021;22:9097.
12. Yousry C, Saber MM, Abd Elsalam WH. A cosmeceutical topical water in oil Nanoemulsion of natural bioactives: Design of Experiment, in vitro characterization, and in vivo skin performance against UVB irradiation induced skin damages. *Int J Nanomedicine*. 2022;17:2995-3012.
13. Marine Casado R, Teichenne J, Tobajas Y, et al. Pomegranate natural extract Pomanox((R)) positively modulates skin health related parameters in normal and UV induced photoaging conditions in Hs68 human fibroblast cells. *Int J Food Sci Nutr*. 2023;74:51-63.
14. Lin H, Cheng KC, Lin JA, et al. Pholiota nameko polysaccharides protect against ultraviolet A induced Photoaging by regulating matrix Metalloproteinases in human dermal fibroblasts. *Antioxidants (Basel)*. 2022;11:739.
15. Rivera Yanez CR, Ruiz Hurtado PA, Mendoza Ramos MI, et al. Flavonoids present in propolis in the battle against photoaging and psoriasis. *Antioxidants (Basel)*. 2021;10:2014.
16. Carneiro Ferreira I, Pereira da Silva V, Vilvert JC, de Franca Souza F, de Freitas ST, Dos Santos Lima M. Brazilian varieties of acerola (Malpighia emarginata DC.) produced under tropical semi arid conditions: bioactive phenolic compounds, sugars, organic acids, and antioxidant capacity. *J Food Biochem*. 2021;23:e13829.
17. Belwal T, Devkota HP, Hassan HA, et al. Phytopharmacology of acerola (*Malpighia* spp.) and its potential as a functional food. *Trends Food Sci Technol*. 2018;74:99-106.
18. Hanamura T, Uchida E, Aoki H. Skin lightening effect of a polyphenol extract from acerola (*Malpighia emarginata* DC.) fruit on UV induced pigmentation. *Biosci Biotechnol Biochem*. 2008;72:3211-3218.
19. Yan L, Zhou G, Shahzad K, et al. Research progress on the utilization technology of broccoli stalk, leaf resources, and the mechanism of action of its bioactive substances. *Front Plant Sci*. 2023;14:1138700.
20. Villarroel VA, Kerns ML, Wang R, et al. 603 randomized, split body, blinded clinical study of topical sulforaphane rich broccoli sprout extract on photodamaged skin. *J Invest Dermatol*. 2018;138:65.
21. Zhang YQ, Guan L, Zhong ZY, et al. The anti-inflammatory effect of cherry blossom extract (*Prunus yedoensis*) used in soothing skincare product. *Int J Cosmet Sci*. 2014;36:527-530.
22. Wang Y, Li W, Xu S, et al. Protective skin aging effects of cherry blossom extract (*Prunus yedoensis*) on oxidative stress and apoptosis in UVB irradiated HaCaT cells. *Cytotechnology*. 2019;71:475-487.
23. Blanco M, Sanz N, Sánzhez AC, Correa B, Pérez Martín RI, Sotelo CG. Molecular weight analysis of blue shark (*Prionace glauca*) collagen hydrolysates by GPC LS; effect of high molecular weight hydrolysates on fibroblast cultures: mRNA collagen type I expression and synthesis. *Int J Mol Sci*. 2021;23:32.
24. Liu Y, Su G, Zhou F, Zhang J, Zheng L, Zhao M. Protective effect of bovine elastin peptides against Photoaging in mice and identification of novel Antiphotoaging peptides. *J Agric Food Chem*. 2018;66:10760-10768.
25. Ghafoor K, Ahmed IAM, Doğu S, et al. The effect of heating temperature on Total phenolic content, antioxidant activity, and phenolic compounds of plum and Mahaleb fruits. *Int J Food Eng*. 2019;15:7406.
26. Grande T, Souid A, Ciardi M, et al. Evaluation of antioxidant and antimicrobial activities of whole flours obtained from different species of Triticum genus. *Eur Food Res Technol*. 2023;249:1575-1587.
27. Serafini MR, Detoni CB, Menezes PDP, et al. UVA UVB Photoprotective activity of topical formulations ContainingMorinda citrifoliaExtract. *Biomed Res Int*. 2014;2014:1-10.
28. Zhang M, Zhang T, Tang Y, Ren G, Zhang Y, Ren X. Concentrated growth factor inhibits UVA induced photoaging in human dermal fibroblasts via the MAPK/AP 1 pathway. *Biosci Rep*. 2020;40:BSR20193566.
29. Deng M, Xu Y, Yu Z, et al. Protective effect of fat extract on UVB induced Photoaging in vitro and in vivo. *Oxid Med Cell Longev*. 2019;2019:6146942.
30. Jung JM, Choi JK, Kwon OY, Lee SH. Anti Photoaging activity of *Scutellaria barbata* D. Don (family Lamiaceae) on ultraviolet B irradiated NIH 3T3 skin fibroblast and SKH 1 hairless mouse. *Molecules*. 2022;27:3803.

31. Sun Q, Liu P, You S, et al. Protective effects of LPL EPS 02 on human dermal fibroblasts damaged by UVA radiation. *J Funct Foods*. 2021;83:104544.
32. Tan CYR, Tan CL, Chin T, et al. Nicotinamide prevents UVB and oxidative stress–induced Photoaging in human primary keratinocytes. *J Invest Dermatol*. 2022;142:1670-1681.e12.
33. Geng R, Kang SG, Huang K, Tong T. Boosting the photoaged skin: the potential role of dietary components. *Nutrients*. 2021;13:1691.
34. Sun W, He J, Zhang Y, He R, Zhang X. Comprehensive functional evaluation of novel collagen for the skin protection in human fibroblasts and keratinocytes. *Biosci Biotechnol Biochem*. 2023;87:724-735.
35. Liu Z, Li Y, Song H, et al. Collagen peptides promote photoaging skin cell repair by activating the TGF beta/Smad pathway and depressing collagen degradation. *Food Funct*. 2019;10:6121-6134.
36. Wei G, Xu Q, Liu L, et al. LY2109761 reduces TGF β1induced collagen production and contraction in hypertrophic scar fibroblasts. *Arch Dermatol Res*. 2018;310:615-623.
37. Bouatenin KMJP, Camara F, Tohoyessou YMG, et al. Contribution to the improvement of the nutritional and functional properties of bread by incorporating cinnamon powder (*Cinnamomum verum*). *Food Sci Nutr*. 2023;11:6241-6248.
38. Alsuhaibani AM, Alkuraieef AN, Aljobair MO, Alshawi AH, Lucarini M. Technological, sensory, and hypoglycemic effects of quinoa flour incorporation into biscuits. *J Food Qual*. 2022;2022:1-7.
39. Hong H, Fan H, Chalamaiah M, Wu J. Preparation of low molecular weight, collagen hydrolysates (peptides): current progress, challenges, and future perspectives. *Food Chem*. 2019;301:125222.
40. Bosch R, Philips N, Suárez Pérez J, et al. Mechanisms of Photoaging and cutaneous Photocarcinogenesis, and Photoprotective strategies with phytochemicals. *Antioxidants*. 2015;4:248-268.
41. Sukhikh S, Noskova S, Ivanova S, et al. Comparative analysis of collagen containing waste biodegradation, amino acid, peptide and carbohydrate composition of hydrolysis products. *Applied Sciences*. 2021;11:2507-2526.
42. Kwon YW, Heo SC, Lee TW, et al. N acetylated Proline glycine Proline accelerates cutaneous wound healing and neovascularization by human endothelial progenitor cells. *Sci Rep*. 2017;7:43057.
43. Kwon KC, Won JG, Seo JH, et al. Effects of arginine glutamate (RE: pair) on wound healing and skin elasticity improvement after CO2 laser irradiation. *J Cosmet Dermatol*. 2022;21:5037-5048.
44. Mirzaee H, Ahmadi Gavlighi H, Nikoo M, Udenigwe CC, Khodaiyan F. Relation of amino acid composition, hydrophobicity, and molecular weight with antidiabetic, antihypertensive, and antioxidant properties of mixtures of corn gluten and soy protein hydrolysates. *Food Sci Nutr*. 2022;11:1257-1271.
45. Kim D, Choi EH, Lee JY, et al. Glucocerebroside containing Milk concentrated powder suppresses oxidative stress and Photoaging in the skin of hairless mice. *Antioxidants (Basel)*. 2022;11:1804.
46. Jin Y, Cheng X, Huang X, et al. The role of Hrd1 in ultraviolet (UV) radiation induced photoaging. *Aging (Albany N Y)*. 2020;12:21273-21289.
47. Mo Q, Li S, You S, et al. Puerarin reduces oxidative damage and Photoaging caused by UVA radiation in human fibroblasts by regulating Nrf2 and MAPK signaling pathways. *Nutrients*. 2022;14:4724.
48. Bugara B, Konieczny P, Wolnicka Glubisz A, et al. MCPIP1 contributes to the inflammatory response of UVB treated keratinocytes. *J Dermatol Sci*. 2017;87:10-18.
49. Matsuura Hachiya Y, Arai KY, Muraguchi T, Sasaki T, Nishiyama T. Type IV collagen aggregates promote keratinocyte proliferation and formation of the epidermal layer in human skin equivalents. *Exp Dermatol*. 2018;27:443-448.
50. De Jager TL, Cockrell AE, Du Plessis SS. Ultraviolet light induced generation of reactive oxygen species. *Adv Exp Med Biol*. 2017;996:15-23.
51. Hudson L, Rashdan E, Bonn CA, Chavan B, Rawlings D, Birch Machin MA. Individual and combined effects of the infrared, visible, and ultraviolet light components of solar radiation on damage biomarkers in human skin cells. *FASEB J*. 2020;34:3874-3883.
52. Bavkar LN, Patil RS, Rooge SB, Nalawade ML, Arvindekar AU. Acceleration of protein glycation by oxidative stress and comparative role of antioxidant and protein glycation inhibitor. *Mol Cell Biochem*. 2019;459:61-71.
53. Choi HJ, Alam MB, Baek ME, Kwon YG, Lim JY, Lee SH. Protection against UVB induced Photoaging by Nypa fruticans via inhibition of MAPK/AP 1/MMP1 signaling. *Oxid Med Cell Longev*. 2020;2020:2905362.
54. Yun MS, Kim C, Hwang JK. Agastache rugosa Kuntze attenuates UVB induced Photoaging in hairless mice through the regulation of MAPK/AP 1 and TGF beta/ Smad pathways. *J Microbiol Biotechnol*. 2019;29:1349-1360.
55. Amano S. Characterization and mechanisms of photoageing related changes in the skin. Damages of basement membrane and dermal structures. *Exp Dermatol*. 2016;25:14-19.
56. Son DJ, Jung JC, Choi YM, Ryu HY, Lee S, Davis BA. Wheat extract oil (WEO) attenuates UVB induced Photoaging via collagen synthesis in human keratinocytes and hairless mice. *Nutrients*. 2020;12:300.
57. Rock K, Grandoch M, Majora M, Krutmann J, Fischer JW. Collagen fragments inhibit hyaluronan synthesis in skin fibroblasts in response to ultraviolet B (UVB): new insights into mechanisms of matrix remodeling. *J Biol Chem*. 2011;286:18268-18276.
58. Xia Y, Yu E, Li Z, et al. Both TGF beta1 and Smad4 regulate type I collagen expression in the muscle of grass carp, *Ctenopharyngodon idella*. *Fish Physiol Biochem*. 2021;47:907-917.
59. Oh JH, Kim J, Karadeniz F, et al. Santamarine shows anti Photoaging properties via inhibition of MAPK/AP 1 and stimulation of TGF β/Smad signaling in UVA irradiated HDFs. *Molecules*. 2021;26:3585.
60. Kim YH, Cho A, Kwon SA, et al. Potential Photoprotective effect of dietary corn silk extract on ultraviolet B induced skin damage. *Molecules*. 2019;24:2587.

How to cite this article: Guo K, Zheng L, Zeng X, Huang G, Meng L, Yin Y. Compound collagen peptide powder improves skin photoaging by reducing oxidative stress and activating TGF-β1/Smad pathway. *Photochem Photobiol*. 2024;00:1-19. doi:10.1111/php.13940